1993009 3383 L-33
Acc No. L5H04

NATIONAL ADVISORY COMMITTEE FOR AERONAUTICS

WARTIME REPORT

ORIGINALLY ISSUED

October 1945 as
[redacted] Report L5H04

COLUMN AND PLATE COMPRESSIVE STRENGTHS OF AIRCRAFT STRUCTURAL MATERIALS

EXTRUDED R303-T ALUMINUM ALLOY

By George J. Heimerl and Douglas P. Fay

Langley Memorial Aeronautical Laboratory
Langley Field, Va.

WASHINGTON

NACA WARTIME REPORTS are reprints of papers originally issued to provide rapid distribution of advance research results to an authorized group requiring them for the war effort. They were previously held under a security status but are now unclassified. Some of these reports were not technically edited. All have been reproduced without change in order to expedite general distribution.

NATIONAL ADVISORY COMMITTEE FOR AERONAUTICS

[redacted] REPORT

COLUMN AND PLATE COMPRESSIVE STRENGTHS OF AIRCRAFT STRUCTURAL MATERIALS

EXTRUDED R303-T ALUMINUM ALLOY

By George J. Heimerl and Douglas P. Fay

SUMMARY

Column and plate compressive strengths of extruded R303-T aluminum alloy were determined both within and beyond the elastic range from tests of thin-strip columns and local-instability tests of H-, Z-, and channel-section columns. These tests are part of an extensive research investigation to provide data on the structural strength of various aircraft materials. The results are presented in the form of curves and charts that are suitable for use in the design and analysis of aircraft structures.

INTRODUCTION

Column and plate members in an aircraft structure are the basic elements that fail by instability. For the design of structurally efficient aircraft, the strength of these elements must be known for the various aircraft materials. An extensive research program has therefore been undertaken at the Langley Memorial Aeronautical Laboratory to establish the column and plate compressive strengths of a number of the alloys available for use in aircraft structures. Parts of this investigation have already been completed; the alloys already investigated include 24S-T and 17S-T aluminum-alloy sheet and extruded 75S-T and 24S-T aluminum alloys (references 1 to 4, respectively).

The results of tests to determine the column and plate compressive strengths of extruded R303-T aluminum alloy are presented herein.

SYMBOLS

L	length of column
ρ	radius of gyration
c	fixity coefficient used in Euler column formula
$\frac{L}{\rho\sqrt{c}}$	effective slenderness ratio of column
b_F, t_F	width and thickness, respectively, of flange of H-, Z-, or channel section (see fig. 1)
b_W, t_W	width and thickness, respectively, of web of H-, Z-, or channel section (see fig. 1)
r	corner radius (see fig. 1)
k_W	nondimensional coefficient used with b_W and t_W in plate-buckling formula (see figs. 2 and 3)
E_c	modulus of elasticity in compression, taken as 10,500 ksi for extruded R303-T aluminum alloy
τ	nondimensional coefficient (The value of τ is so determined that, when the effective modulus of elasticity τE_c is substituted for E_c in the equation for elastic buckling of columns, the computed critical stress agrees with the experimentally observed value. The coefficient τ is equal to unity within the elastic range and decreases with increasing stress beyond the elastic range.)
η	nondimensional coefficient for compressed plates corresponding to τ for columns
μ	Poisson's ratio, taken as 0.3 for extruded R303-T aluminum alloy
σ_{cr}	critical compressive stress
$\bar{\sigma}_{max}$	average compressive stress at maximum load
σ_{cy}	compressive yield stress

METHODS OF TESTING AND ANALYSIS

All tests were made in hydraulic testing machines accurate within three-fourths of 1 percent. The methods of testing and analysis developed for this research program (see reference 1) are briefly summarized as follows:

The compressive stress-strain curves for the extrusions, which identify the material for correlation with its column and plate compressive strengths, were obtained for the with-grain direction from tests of single-thickness compression specimens cut from the flanges and web at both ends of the extruded H-sections. These tests were made in a compression fixture of the Montgomery-Templin type, which provides lateral support to the specimens through closely spaced rollers. (See reference 6 for the technique in using this type of fixture.)

The column strength and the associated effective column modulus were obtained for the with-grain direction by the use of the method presented in reference 7, in which thin-strip columns of the material were tested with the ends clamped in fixtures that provide a high degree of end restraint. The fixtures used have been improved and the method of analysis has been modified since publication of reference 7. The method now used results in a column curve representative of nearly perfect column specimens. In addition, the method now takes into account the fact that columns of the dimensions tested are actually plates with two free edges. These columns were cut from the flanges of the extruded H-section adjacent to the fillet at the junction of the web and flange.

The plate compressive strength was obtained from compression tests of H-, Z-, and channel-section columns so proportioned as to develop local instability, that is, instability of the plate elements. (See fig. 4.) Extruded H-sections of three different web widths were tested; the flange widths for each were varied by milling off parts of the flanges. The flanges of some of the H-section extrusions were removed in such a way as to make Z- or channel sections as desired; the flange widths of the Z- and channel-section columns were varied in the same manner as the flange widths for the H-section columns. The lengths of the columns were selected in accordance with the principles in reference 8. The columns were tested with the ends ground flat and square and bearing directly against

the testing-machine heads. In these local-instability tests, measurements were taken of the cross-sectional distortion, and the critical stress was determined as the stress at the point near the top of the knee of the stress-distortion curve where a marked increase in distortion first occurred with small increase in stress.

The method of analysis presented herein differs from that presented in reference 1 in the use of the inside face dimensions to define b_F and b_W in the evaluation of σ_{cr}/η by means of the equations and curves of figures 2 and 3. This definition of b_F and b_W for extruded sections with small fillets was previously used in references 3 and 4 in order that the theoretical and experimental buckling stresses would agree within the elastic range. For formed Z- and channel sections with an inside bend radius of three times the sheet thickness (references 1 and 2), b_F and b_W were defined as center-line widths with square corners assumed.

RESULTS AND DISCUSSION

Compressive Properties

Figure 5 summarizes the compressive stress-strain curves that apply to the extruded R303-T aluminum alloy used in this investigation. The variation in compressive yield stress shown by the dashed curves in figure 5 for both the flange and web indicates the average differences that were found to exist between the two ends of the 20-foot extrusions. The results of a single survey made over the cross section of one extrusion (fig. 6) revealed but little variation in the compressive yield stress over the width of a flange or a web. At a given cross section, the web tended always to have a lower compressive yield stress than the flange.

Column and Plate Compressive Strengths

Because the compressive properties of an extruded aluminum alloy may vary considerably, the data and charts of this report should not be used for design purposes for extrusions of R303-T aluminum alloy that have appreciably different compressive properties from those reported

herein, unless a suitable method is devised for adjusting test results to account for variations in material properties. The results of the column and local-instability tests of extruded R303-T aluminum alloy are summarized herein; a discussion of the basic relationships is given in reference 1.

Column strength.- The column curve of figure 7 shows the results of tests of thin-strip columns loaded in the with-grain direction. The reduction of the effective modulus of elasticity τE_c with the increase in column stress is indicated by the variation of τ with stress shown in figure 8.

Plate compressive strength.- The results of the local-instability tests of the H-, Z-, and channel-section columns used to determine the plate compressive strength are given in tables 1, 2, and 3, respectively. The plate-buckling curves, analogous to the column curve of figure 7, are shown in figure 9. The reduction of the effective modulus of elasticity ηE_c with increase in stress is indicated by the variation of η with stress, which is shown together with the curve for τ in figure 8. In this figure, the τ-curve crosses the η-curves because the extruded H-, Z-, and channel-section columns used to obtain the η-curves apparently had an appreciable degree of imperfection. This imperfection probably caused the η-curves to deviate from unity at a lower stress than that for the τ-curve, which is representative of nearly perfect columns.

The variation of the actual critical stress σ_{cr} with the theoretical critical stress σ_{cr}/η computed for elastic buckling by means of the formula and curves of figures 2 and 3 is shown in figure 10.

In order to illustrate the difference between the critical stress σ_{cr} and the average stress at maximum load $\bar{\sigma}_{max}$, the variation of σ_{cr} with $\sigma_{cr}/\bar{\sigma}_{max}$ is shown in figure 11. Because values of $\bar{\sigma}_{max}$ may be required in strength calculations, the variation of $\bar{\sigma}_{max}$ with σ_{cr}/η is shown in figure 12.

Figures 9 to 12 show that the data for H-sections describe different curves from those indicated for Z- and channel sections. One of the reasons why higher values

of $\overline{\sigma}_{max}$ were obtained for H-sections than for Z- or channel sections for a given value of σ_{cr}/η (fig. 12) may be the fact that the high-strength material in the flanges (see fig. 6) forms a higher percentage of the total cross-sectional area for the H-section than for the Z- or channel section. For the H-section, $\overline{\sigma}_{max}$ is increased over the value of $\overline{\sigma}_{max}$ for the Z- or channel section for the entire stress range covered in these tests (fig. 12) whereas σ_{cr} is increased only beyond the elastic range (fig. 10).

Langley Memorial Aeronautical Laboratory
National Advisory Committee for Aeronautics
Langley Field, Va.

REFERENCES

1. Lundquist, Eugene E., Schuette, Evan H., Heimerl, George J., and Roy, J. Albert: Column and Plate Compressive Strengths of Aircraft Structural Materials. 24S-T Aluminum-Alloy Sheet. NACA ARR No. L5F01, 1945.

2. Heimerl, George J., and Roy, J. Albert: Column and Plate Compressive Strengths of Aircraft Structural Materials. 17S-T Aluminum-Alloy Sheet. NACA ARR No. L5F08, 1945.

3. Heimerl, George J., and Roy, J. Albert: Column and Plate Compressive Strengths of Aircraft Structural Materials. Extruded 75S-T Aluminum Alloy. NACA ARR No. L5F08a, 1945.

4. Heimerl, George J., and Roy, J. Albert: Column and Plate Compressive Strengths of Aircraft Structural Materials. Extruded 24S-T Aluminum Alloy. NACA ARR No. L5F08b, 1945.

5. Kroll, W. D., Fisher, Gordon P., and Heimerl, George J. Charts for Calculation of the Critical Stress for Local Instability of Columns with I-, Z-, Channel, and Rectangular-Tube Section. NACA ARR No. 3K04, 1943.

6. Kotanchik, Joseph N., Woods, Walter, and Weinberger, Robert A.: Investigation of Methods of Supporting Single-Thickness Specimens in a Fixture for Determination of Compressive Stress-Strain Curves. NACA RB No. L5E15, 1945.

7. Lundquist, Eugene E., Rossman, Carl A., and Houbolt, John C.: A Method for Determining the Column Curve from Tests of Columns with Equal Restraints against Rotation on the Ends. NACA TN No. 903, 1943.

8. Heimerl, George J., and Roy, J. Albert: Determination of Desirable Lengths of Z- and Channel-Section Columns for Local-Instability Tests. NACA RB No. L4H10, 1944.

TABLE 1.- DIMENSIONS AND TEST RESULTS FOR EXTRUDED H-SECTION COLUMNS THAT DEVELOP LOCAL INSTABILITY

Column	t_W (in.)	t_F (in.)	b_W (in.)	b_F (in.)	L (in.)	L/b_W	t_W/t_F	b_W/t_W	b_F/b_W	k_W (fig. 2)	$\frac{b_W}{t_W}\sqrt{\frac{12(1-\mu^2)}{k_W}}$	$\frac{\sigma_{cr}}{\eta}$ (ksi) (a)	σ_{cr} (ksi)	$\bar{\sigma}_{max}$ (ksi)	$\frac{\sigma_{cr}}{\bar{\sigma}_{max}}$
1a	0.124	0.125	1.64	0.83	5.98	3.6	0.994	13.24	0.504	2.63	27.0	142.4	76.8	77.6	0.990
1b	.124	.124	1.63	.83	6.10	3.7	.999	13.19	.508	2.56	27.2	139.6	76.1	77.2	.986
1c	.124	.122	1.64	.83	6.03	3.7	1.011	13.25	.506	2.55	27.4	137.8	75.5	77.5	.974
2a	.124	.122	1.63	.90	6.95	4.3	1.017	13.14	.555	2.18	29.4	119.8	74.9	76.2	.983
2b	.124	.122	1.64	.90	7.00	4.3	1.013	13.25	.551	2.22	29.4	120.0	74.2	76.4	.971
2c	.123	.122	1.63	.90	7.00	4.3	1.012	13.21	.554	2.20	29.4	119.6	74.0	75.8	.976
3a	.123	.122	1.64	.99	7.92	4.8	1.011	13.26	.608	1.88	32.0	101.5	72.3	73.4	.985
3b	.124	.122	1.64	.99	7.84	4.8	1.011	13.26	.606	1.89	31.9	102.0	72.1	73.1	.986
3c	.123	.122	1.64	.99	7.87	4.8	1.009	13.28	.607	1.88	32.0	101.1	72.5	73.5	.986
4a	.124	.122	1.64	1.08	8.72	5.3	1.017	13.20	.661	1.62	34.3	88.3	69.9	70.7	.989
4b	.124	.122	1.65	1.08	8.72	5.3	1.012	13.29	.656	1.64	34.3	88.1	70.0	71.3	.982
4c	.124	.123	1.64	1.08	8.75	5.3	1.008	13.28	.658	1.65	34.2	88.8	70.4	71.6	.983
5a	.123	.121	1.65	1.18	10.08	6.1	1.017	13.37	.714	1.41	37.2	74.8	67.0	68.5	.978
5b	.123	.122	1.66	1.18	10.08	6.1	1.011	13.49	.709	1.43	37.3	74.6	67.4	68.0	.991
5c	.123	.122	1.66	1.18	10.06	6.1	1.012	13.46	.710	1.42	37.3	74.4	66.1	67.5	.979
6a	.124	.122	1.64	1.26	10.40	6.3	1.016	13.23	.767	1.24	39.3	67.2	64.7	65.3	.991
6b	.123	.122	1.64	1.26	10.40	6.4	1.010	13.29	.769	1.25	39.3	67.2	65.1	65.9	.988
6c	.124	.122	1.65	1.26	10.40	6.3	1.012	13.32	.765	1.25	39.4	66.9	64.1	65.7	.976
7a	.124	.123	1.64	1.36	10.80	6.6	1.008	13.27	.826	1.10	41.8	59.3	60.2	61.8	.974
7b	.124	.122	1.64	1.36	10.80	6.6	1.016	13.19	.827	1.10	41.6	60.0	59.6	60.9	.979
7c	.123	.121	1.65	1.36	10.81	6.6	1.009	13.44	.825	1.11	42.2	58.3	59.5	62.6	.950
8a	.130	.122	2.23	1.12	10.69	4.8	1.068	17.11	.503	2.46	36.0	79.7	65.7	67.1	.979
8b	.130	.122	2.24	1.12	10.68	4.8	1.064	17.25	.502	2.44	36.5	77.8	66.3	67.4	.984
8c	.130	.123	2.23	1.12	10.59	4.8	1.057	17.13	.503	2.48	35.9	80.2	66.9	68.8	.972
9a	.123	.122	2.26	1.24	11.50	5.1	1.009	18.33	.547	2.25	40.4	63.5	60.2	63.0	.956
9b	.123	.122	2.26	1.24	11.58	5.1	1.006	18.37	.550	2.24	40.6	63.0	60.5	62.8	.963
10a	.130	.122	2.23	1.35	12.58	5.6	1.061	17.23	.606	1.79	42.6	57.2	55.8	57.6	.969
10b	.129	.121	2.26	1.36	12.54	5.6	1.070	17.50	.601	1.80	43.1	55.8	55.6	57.4	.969
10c	.129	.121	2.26	1.36	12.55	5.6	1.073	17.46	.600	1.80	43.0	56.0	55.7	57.7	.965
11a	.130	.122	2.25	1.47	13.26	5.9	1.063	17.30	.654	1.56	45.8	49.5	48.7	54.4	.895
11b	.129	.121	2.25	1.48	13.28	5.9	1.069	17.50	.656	1.54	46.6	47.7	48.0	54.5	.881
11c	.130	.122	2.26	1.48	13.35	5.9	1.067	17.37	.655	1.58	45.7	49.7	48.4	54.6	.886
12a	.130	.122	2.25	1.60	13.80	6.1	1.061	17.36	.709	1.37	49.0	43.1	42.3	51.8	.817
12b	.130	.121	2.26	1.59	13.84	6.1	1.073	17.44	.705	1.37	49.2	42.7	42.0	52.1	.806
13a	.128	.123	2.25	1.84	15.06	6.7	1.042	17.52	.816	1.09	55.5	33.7	30.3	48.7	.622
13b	.129	.121	2.26	1.84	14.57	6.5	1.059	17.55	.814	1.09	55.5	33.6	31.1	49.6	.627
14a	.124	.124	2.75	1.11	11.47	4.2	.998	22.11	.403	3.56	38.7	69.1	62.2	63.6	.978
14b	.124	.124	2.75	1.10	11.50	4.2	1.001	22.12	.399	3.59	38.6	69.6	63.3	63.9	.991
14c	.124	.123	2.76	1.10	11.44	4.1	1.003	22.34	.398	3.60	38.9	68.5	63.2	64.5	.980
15a	.124	.122	2.76	1.23	12.96	4.7	1.018	22.21	.445	3.06	42.0	58.9	55.9	57.7	.969
15b	.124	.124	2.76	1.24	12.98	4.7	.998	22.35	.448	3.09	42.0	58.7	56.1	57.5	.976
15c	.122	.122	2.75	1.23	13.00	4.7	1.001	22.51	.447	3.08	42.4	57.7	55.4	57.0	.972
16a	.121	.121	2.76	1.39	14.40	5.2	.997	22.80	.503	2.62	46.5	47.8	48.0	52.6	.913
16b	.122	.122	2.76	1.38	14.35	5.2	1.005	22.56	.501	2.61	46.1	48.7	48.6	52.9	.919
17a	.123	.122	2.76	1.67	15.18	5.5	1.011	22.45	.607	1.89	54.0	35.6	35.8	48.6	.737
17b	.121	.121	2.76	1.68	15.20	5.5	.994	22.86	.608	1.91	54.6	34.7	35.9	48.6	.739
17c	.121	.122	2.76	1.67	15.16	5.5	.989	22.87	.607	1.93	54.4	35.0	33.8	48.9	.691
18a	.123	.121	2.76	1.96	16.65	6.0	1.016	22.40	.710	1.40	62.6	26.5	26.6	46.7	.570
18b	.122	.122	2.76	1.96	16.63	6.0	1.002	22.62	.710	1.44	62.3	26.7	27.1	46.6	.582
18c	.121	.122	2.77	1.96	16.56	6.0	.993	22.90	.707	1.47	62.4	26.6	27.5	48.1	.572
19a	.123	.121	2.76	2.26	17.77	6.4	1.022	22.39	.820	1.11	70.2	21.0	21.6	44.8	.482
19b	.122	.122	2.76	2.26	17.75	6.4	1.000	22.61	.820	1.13	70.3	21.0	22.6	45.1	.501
19c	.124	.122	2.76	2.26	17.74	6.4	1.016	22.28	.819	1.12	69.6	21.4	22.1	45.7	.484

[a] $\frac{\sigma_{cr}}{\eta} = \frac{k_W \pi^2 E_c t_W^2}{12(1-\mu^2) b_W^2}$, where E_c = 10,500 ksi and μ = 0.3.

NATIONAL ADVISORY
COMMITTEE FOR AERONAUTICS

TABLE 2.- DIMENSIONS AND TEST RESULTS FOR EXTRUDED Z-SECTION COLUMNS THAT DEVELOP LOCAL INSTABILITY

Column	t_W (in.)	t_F (in.)	b_W (in.)	b_F (in.)	L (in.)	L/b_W	t_W/t_F	b_W/t_W	b_F/b_W	k_W (fig. 3)	$\frac{b_W}{t_W}\sqrt{\frac{12(1-\mu^2)}{k_W}}$	$\frac{\sigma_{cr}}{\eta}$ (ksi) (a)	σ_{cr} (ksi)	$\bar{\sigma}_{max}$ (ksi)	$\frac{\sigma_{cr}}{\bar{\sigma}_{max}}$
1a	0.123	0.121	1.63	1.00	6.10	3.7	1.015	13.21	0.613	2.09	30.2	113.7	72.0	74.1	0.972
1b	.123	.121	1.64	.99	6.10	3.7	1.014	13.34	.604	2.14	30.1	114.1	72.3	74.0	.977
1c	.123	.122	1.63	.99	6.08	3.7	1.012	13.19	.612	2.10	30.1	114.5	72.0	73.5	.980
2a	.123	.122	1.65	1.08	6.50	3.9	1.012	13.38	.654	1.87	32.3	99.2	69.5	72.1	.964
2b	.123	.119	1.62	1.08	6.50	4.0	1.026	13.23	.665	1.80	32.6	97.6	69.3	72.3	.959
2c	.123	.122	1.64	1.08	6.40	3.9	1.010	13.33	.658	1.86	32.3	99.4	69.1	72.2	.957
3a	.123	.120	1.65	1.16	6.96	4.2	1.025	13.44	.701	1.64	34.7	86.2	68.1	69.8	.976
3b	.119	.121	1.64	1.16	6.90	4.2	.978	13.84	.707	1.71	35.0	84.8	68.5	71.0	.965
3c	.123	.121	1.64	1.17	6.90	4.2	1.014	13.52	.713	1.62	35.1	84.1	67.5	71.0	.951
4a	.123	.122	1.63	1.35	8.75	5.4	1.008	13.18	.829	1.26	38.8	68.8	60.2	63.6	.947
4b	.123	.122	1.62	1.34	8.72	5.4	1.008	13.14	.828	1.26	38.7	69.2	61.1	64.3	.950
4c	.123	.122	1.63	1.35	8.70	5.4	1.005	13.20	.829	1.26	38.9	68.6	61.0	62.9	.970
5a	.128	.121	2.25	1.00	9.50	4.2	1.062	17.55	.445	3.22	32.3	99.2	69.0	70.3	.982
5b	.128	.121	2.26	1.01	9.50	4.2	1.059	17.66	.448	3.19	32.7	97.1	68.4	69.8	.980
5c	.128	.121	2.26	1.02	9.50	4.2	1.060	17.71	.448	3.19	32.8	96.5	68.2	70.0	.974
6a	.129	.121	2.26	1.57	13.80	6.1	1.063	17.56	.696	1.62	45.6	49.9	45.5	52.7	.863
6b	.128	.122	2.25	1.58	13.68	6.1	1.044	17.62	.703	1.61	45.9	49.2	47.1	53.0	.889
6c	.128	.121	2.26	1.59	13.80	6.1	1.060	17.60	.705	1.56	46.6	47.8	46.9	53.0	.885
7a	.128	.125	2.25	1.83	14.70	6.5	1.031	17.53	.814	1.27	51.4	39.2	36.5	49.8	.733
7b	.128	.122	2.25	1.84	14.68	6.5	1.044	17.64	.818	1.24	52.3	37.8	37.1	50.0	.742
8a	.123	.124	2.77	1.08	11.50	4.2	.993	22.44	.389	3.84	37.8	72.4	62.2	63.4	.981
8b	.123	.123	2.76	1.09	11.50	4.2	.998	22.43	.395	3.78	38.1	71.3	62.2	63.3	.983
8c	.124	.124	2.76	1.08	11.50	4.2	.997	22.33	.392	3.82	37.8	72.7	62.3	63.1	.987
9a	.123	.124	2.76	1.37	14.50	5.3	.998	22.35	.497	2.93	43.1	55.7	53.8	55.2	.975
9b	.123	.123	2.76	1.38	14.56	5.3	1.003	22.38	.500	2.88	43.6	54.6	53.3	54.4	.980
9c	.123	.123	2.76	1.38	14.51	5.3	.997	22.47	.499	2.92	43.4	54.9	53.0	53.8	.985
10a	.124	.120	2.76	1.67	15.50	5.6	1.028	22.31	.604	2.11	50.8	40.2	39.9	48.3	.826
10b	.123	.123	2.75	1.66	15.46	5.6	.998	22.35	.604	2.19	49.9	41.6	40.3	48.8	.826
10c	.125	.124	2.75	1.67	15.50	5.6	1.010	22.06	.605	2.12	50.0	41.3	41.3	49.6	.833
11a	.124	.122	2.79	2.28	17.80	6.4	1.012	22.48	.817	1.29	65.4	24.2	23.5	44.2	.532
11b	.124	.123	2.75	2.28	17.80	6.5	1.010	22.14	.826	1.27	64.9	24.6	24.8	44.3	.560
11c	.122	.123	2.76	2.27	17.28	6.3	.987	22.64	.824	1.32	65.1	24.4	23.5	43.5	.540

a $\frac{\sigma_{cr}}{\eta} = \frac{k_W \pi^2 E_c t_W^2}{12(1-\mu^2)b_W^2}$, where E_c = 10,500 ksi and μ = 0.3.

NATIONAL ADVISORY
COMMITTEE FOR AERONAUTICS

TABLE 3.- DIMENSIONS AND TEST RESULTS FOR EXTRUDED CHANNEL-SECTION COLUMNS THAT DEVELOP LOCAL INSTABILITY

Column	t_W (in.)	t_F (in.)	b_W (in.)	b_F (in.)	L (in.)	L/b_W	t_W/t_F	b_W/t_W	b_F/b_W	k_W (fig. 3)	$\frac{b_W}{t_W}\sqrt{\frac{12(1-\mu^2)}{k_W}}$	$\frac{\sigma_{cr}}{\eta}$ (ksi) (a)	σ_{cr} (ksi)	$\bar{\sigma}_{max}$ (ksi)	$\frac{\sigma_{cr}}{\bar{\sigma}_{max}}$
1a	0.125	0.123	1.64	0.99	6.10	3.7	1.010	13.15	0.605	2.15	29.6	118.0	71.0	74.3	0.956
1b	.124	.123	1.63	.98	6.08	3.7	1.012	13.08	.604	2.16	29.4	119.8	71.2	74.4	.957
1c	.124	.123	1.62	.98	6.20	3.8	1.008	13.12	.606	2.14	29.6	118.0	71.3	75.6	.943
2a	.124	.123	1.61	1.08	6.46	4.0	1.003	13.07	.667	1.84	31.8	102.2	69.3	72.4	.957
2b	.124	.123	1.63	1.08	6.48	4.0	1.006	13.21	.659	1.88	31.8	102.2	69.3	72.0	.963
2c	.123	.121	1.62	1.08	6.48	4.0	1.022	13.12	.665	1.83	32.1	100.9	69.7	72.5	.961
3a	.123	.121	1.62	1.18	6.90	4.3	1.022	13.13	.727	1.56	34.7	85.9	68.1	70.0	.973
3b	.123	.121	1.64	1.18	6.90	4.2	1.020	13.27	.718	1.59	34.8	85.7	66.8	70.6	.946
3c	.123	.121	1.64	1.18	6.90	4.2	1.022	13.31	.718	1.59	34.9	85.2	67.1	70.6	.950
4a	.123	.124	1.63	1.35	8.75	5.4	.996	13.24	.828	1.28	38.7	69.3	62.7	63.6	.986
4b	.123	.124	1.63	1.35	8.75	5.4	.994	13.28	.830	1.28	38.8	68.9	62.2	63.4	.981
5a	.128	.122	2.26	1.01	9.50	4.2	1.050	17.69	.449	3.20	32.7	97.1	68.6	70.0	.980
5b	.129	.122	2.26	1.02	9.50	4.2	1.054	17.60	.450	3.19	32.6	97.7	69.0	70.6	.977
5c	.127	.122	2.26	1.01	9.50	4.2	1.045	17.73	.447	3.20	32.7	96.6	68.3	70.1	.974
6a	.128	.120	2.26	1.59	13.82	6.1	1.068	17.67	.702	1.60	46.2	48.6	47.1	51.8	.909
6b	.129	.124	2.25	1.59	13.80	6.1	1.038	17.53	.704	1.60	45.8	49.4	47.4	51.8	.915
6c	.128	.120	2.25	1.59	13.79	6.1	1.071	17.56	.707	1.54	46.8	47.4	47.3	51.9	.911
7a	.128	.120	2.26	1.84	14.70	6.5	1.068	17.64	.813	1.24	52.3	37.8	36.8	50.3	.732
7b	.128	.120	2.24	1.84	14.69	6.6	1.074	17.45	.820	1.20	52.6	37.4	36.5	50.2	.727
7c	.128	.122	2.26	1.83	14.70	6.5	1.047	17.62	.812	1.25	52.1	38.2	36.9	48.8	.756
8a	.124	.123	2.75	1.08	11.52	4.2	1.003	22.24	.394	3.78	37.8	72.5	63.1	64.8	.974
9a	.124	.122	2.76	1.38	14.46	5.2	1.015	22.26	.501	2.86	43.5	54.8	51.5	53.1	.970
9b	.124	.122	2.76	1.39	14.50	5.3	1.013	22.34	.502	2.86	43.7	54.4	52.0	53.0	.981
9c	.123	.121	2.76	1.38	14.50	5.3	1.015	22.38	.500	2.87	43.6	54.4	52.2	53.4	.978
10a	.124	.121	2.76	1.65	15.50	5.6	1.026	22.17	.600	2.12	50.3	40.9	40.7	48.0	.848
10b	.124	.121	2.76	1.67	15.50	5.6	1.021	22.24	.605	2.11	50.6	40.5	40.6	47.9	.848
10c	.125	.121	2.76	1.67	15.48	5.6	1.029	22.08	.604	2.10	50.3	40.9	40.5	47.5	.853
11a	.122	.121	2.76	2.25	17.73	6.4	1.012	22.63	.816	1.29	65.8	23.9	24.0	42.2	.569
11b	.121	.121	2.76	2.26	17.78	6.4	1.002	22.76	.818	1.30	65.9	23.8	23.6	42.0	.562
11c	.120	.120	2.76	2.26	17.78	6.4	.994	23.09	.819	1.31	66.7	23.3	24.1	44.3	.544

[a] $\frac{\sigma_{cr}}{\eta} = \frac{k_W \pi^2 E_c t_W^2}{12(1-\mu^2) b_W^2}$, where E_c = 10,500 ksi and μ = 0.3.

NATIONAL ADVISORY
COMMITTEE FOR AERONAUTICS

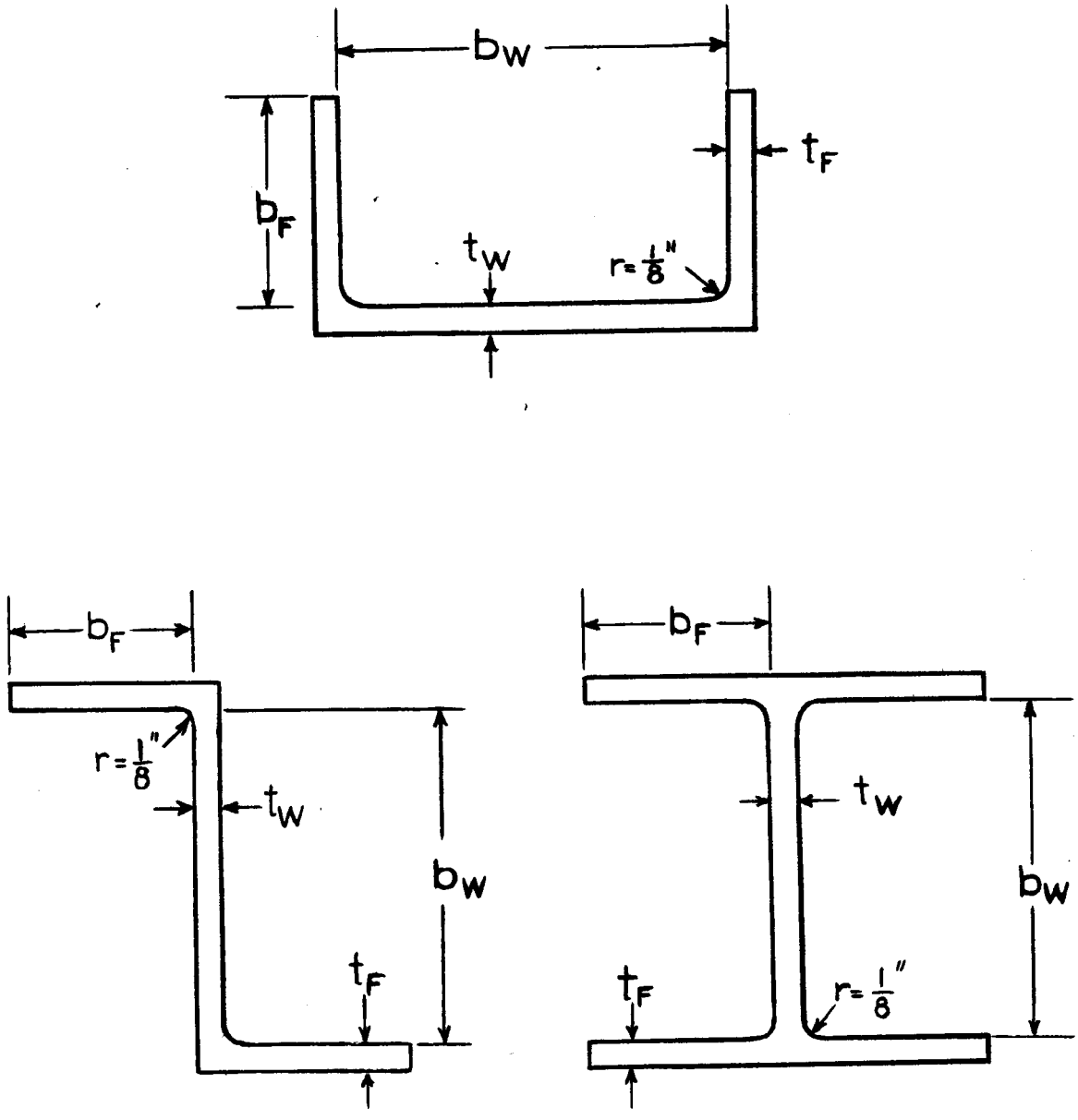

NATIONAL ADVISORY
COMMITTEE FOR AERONAUTICS

Figure 1.- Cross sections of H-, Z-, and channel-section columns.

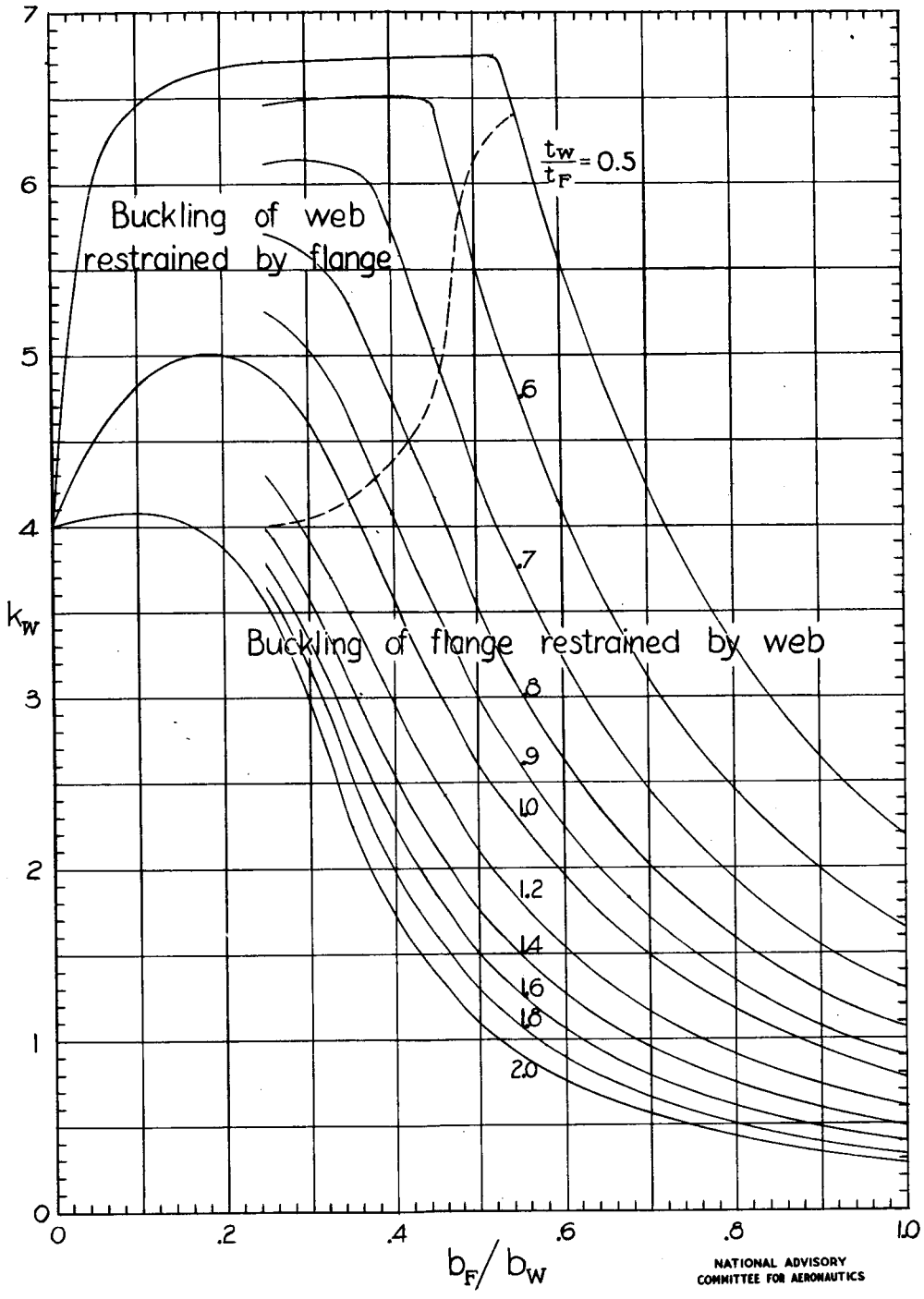

Figure 2.- Values of k_W for H-section columns. (From reference 5.)

$$\frac{\sigma_{cr}}{\eta} = \frac{k_W \pi^2 E_c t_W^2}{12(1-\mu^2) b_W^2}$$

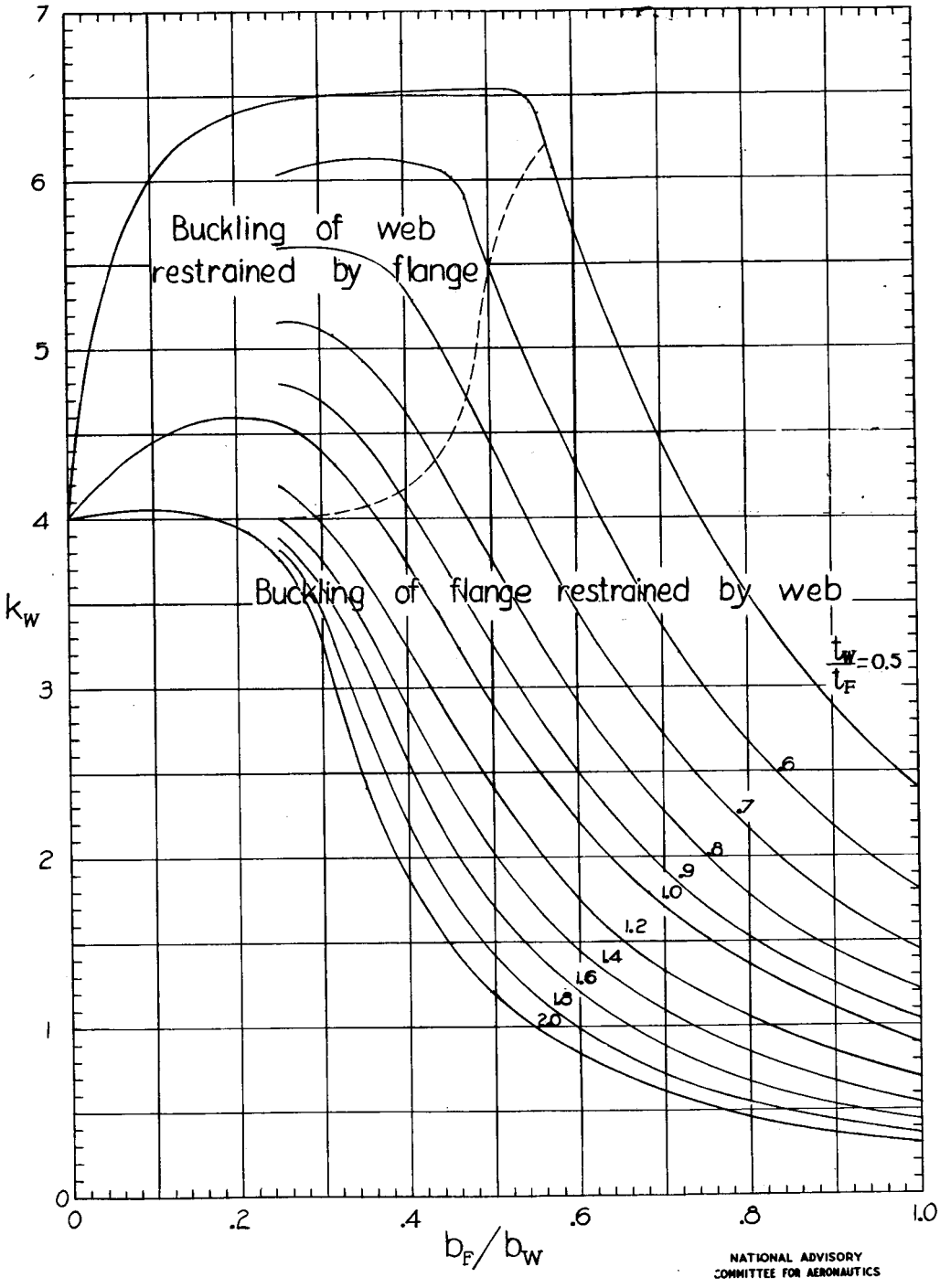

Figure 3.- Values of k_W for Z- and channel-section columns. (From reference 5.)

$$\frac{\sigma_{cr}}{\eta} = \frac{k_W \pi^2 E_c t_W^2}{12(1-\mu^2) b_W^2}$$

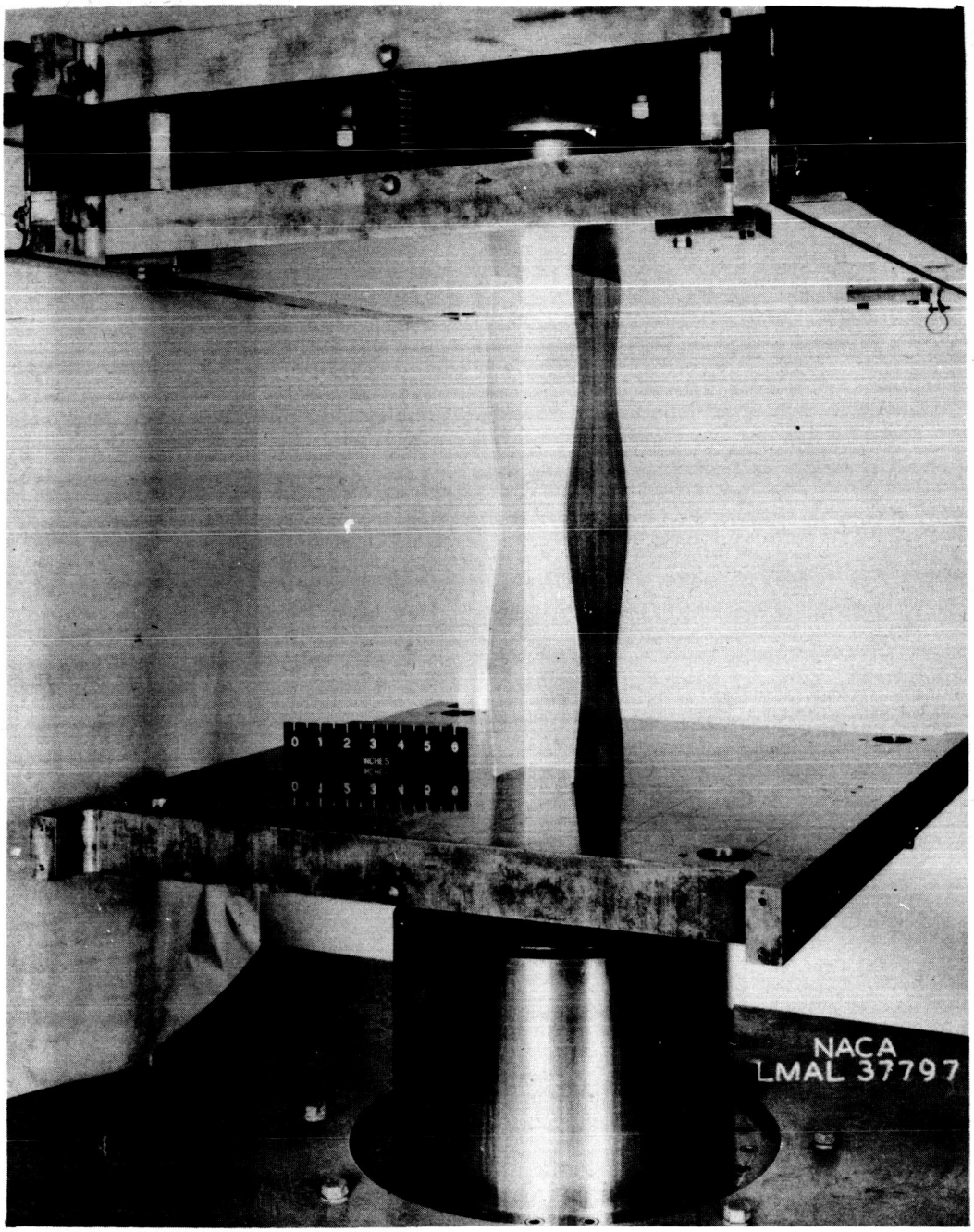

Figure 4.- Local instability of an H-section column.

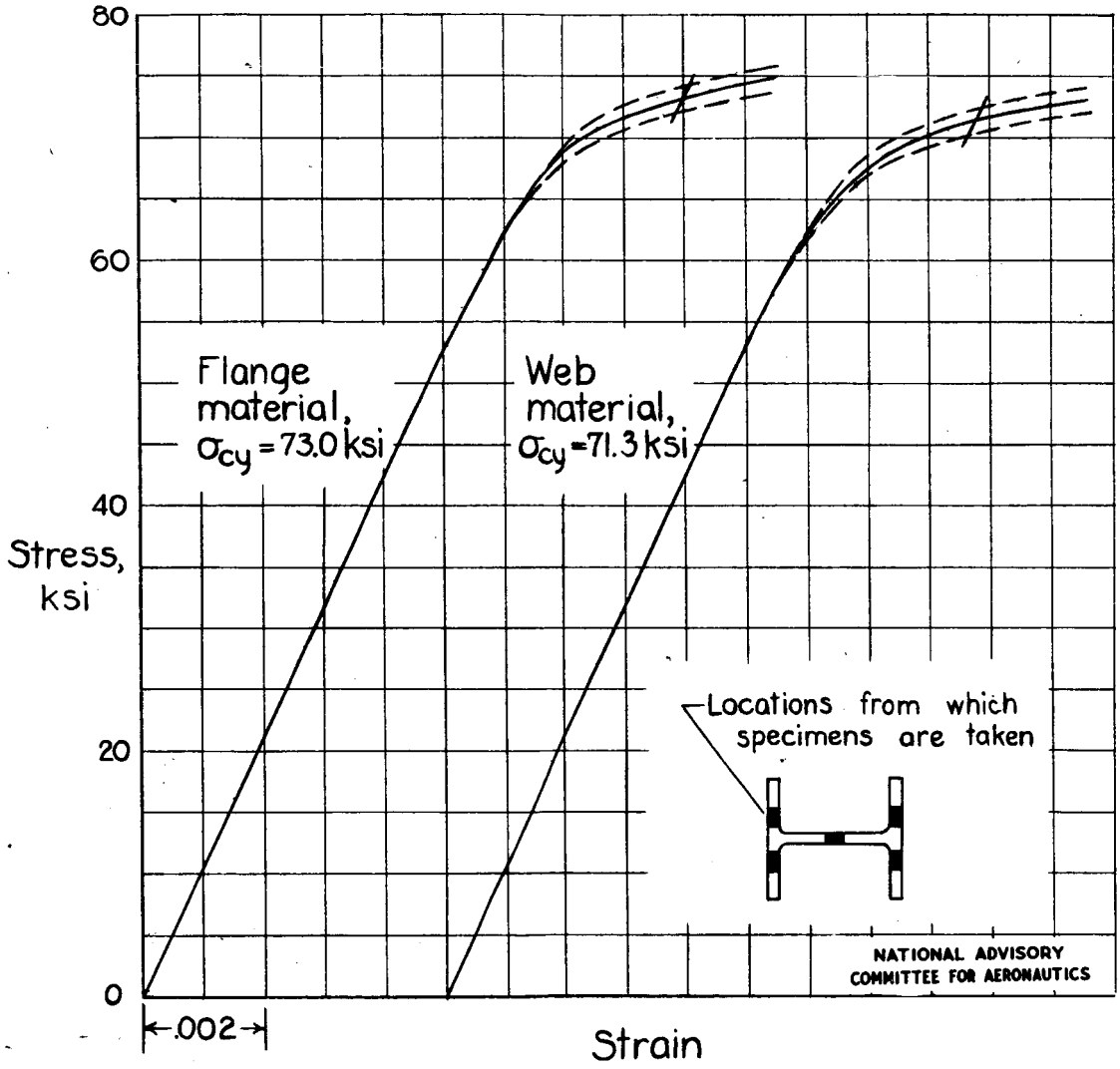

Figure 5.- Compressive stress-strain curves for extruded R303-T aluminum alloy for with-grain direction.

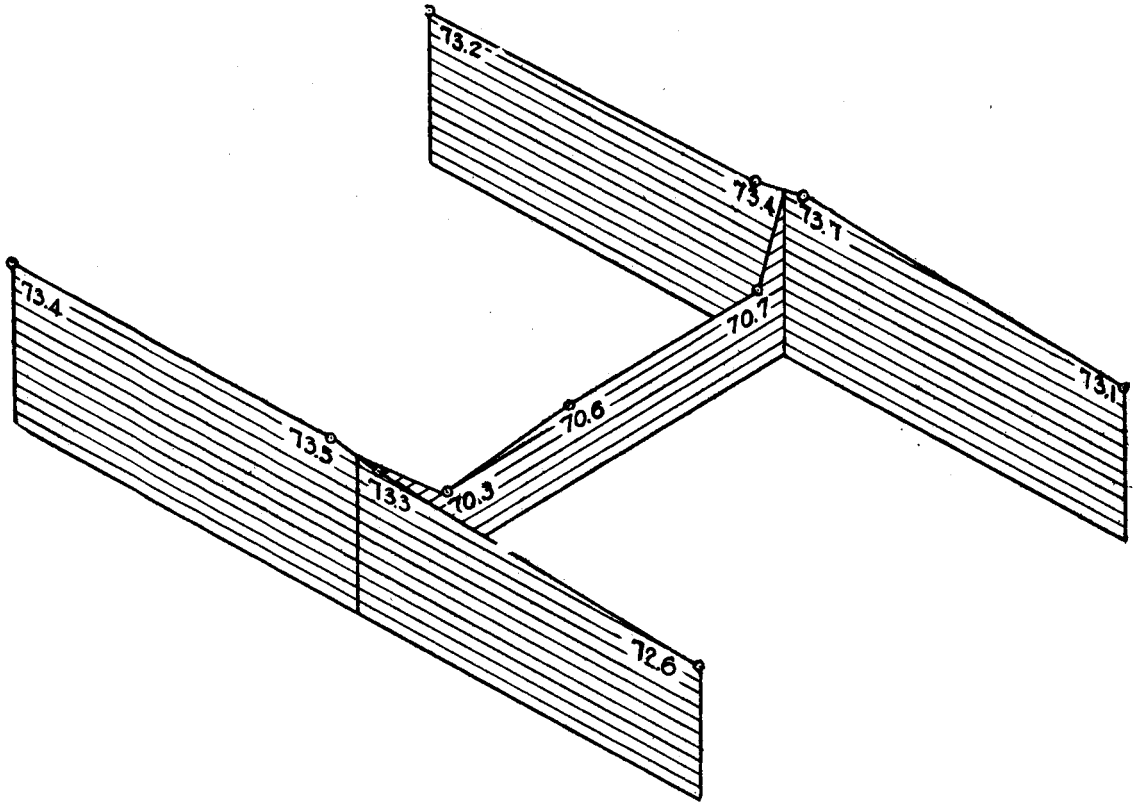

NATIONAL ADVISORY
COMMITTEE FOR AERONAUTICS

Figure 6.– Variation of the compressive yield stress over the cross section of an extruded R303-T aluminum-alloy H-section. (Values in ksi.)

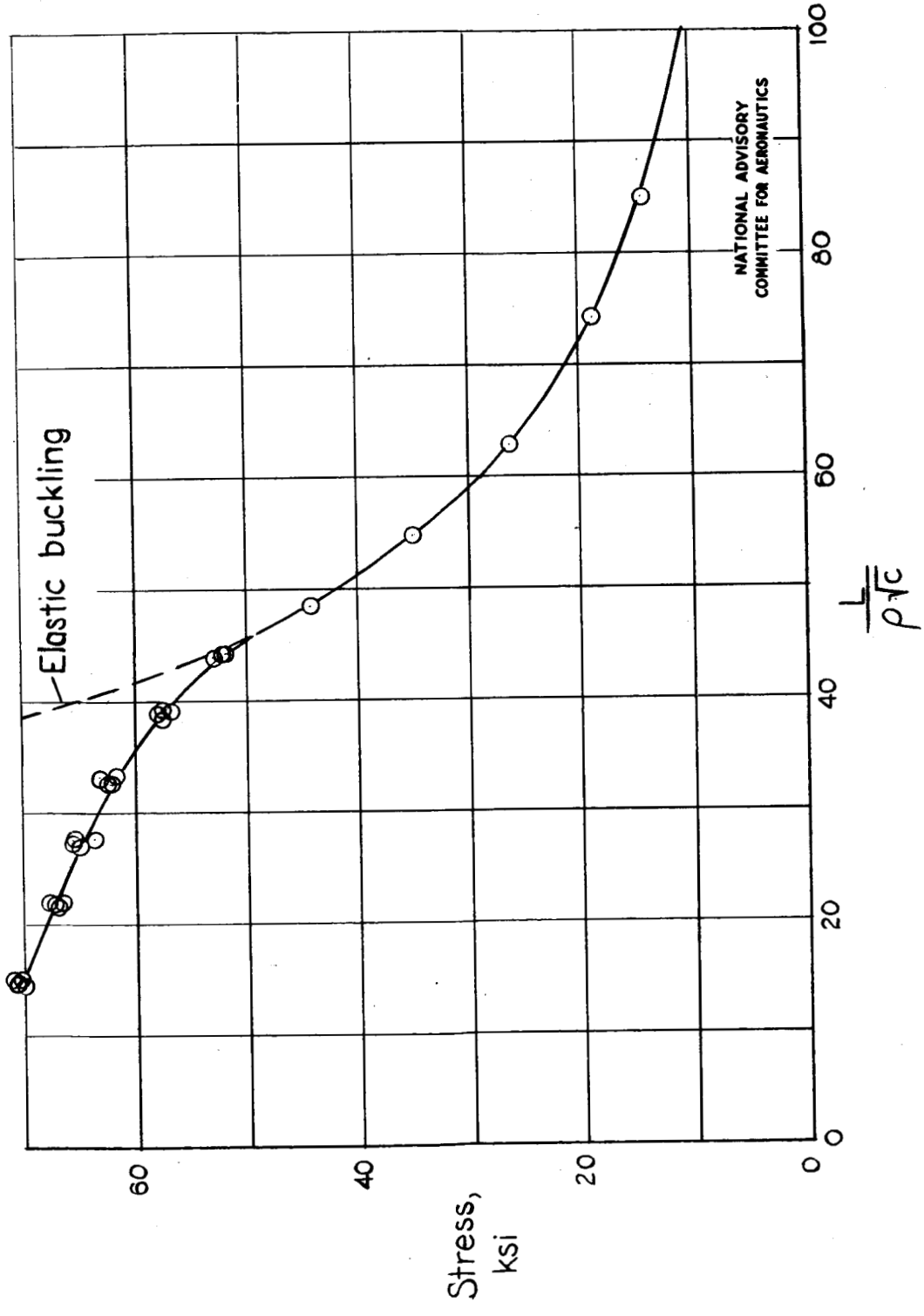

Figure 7.- Column curve for extruded R303-T aluminum alloy obtained from tests of thin-strip columns. $\sigma_{cy} = 73$ ksi.

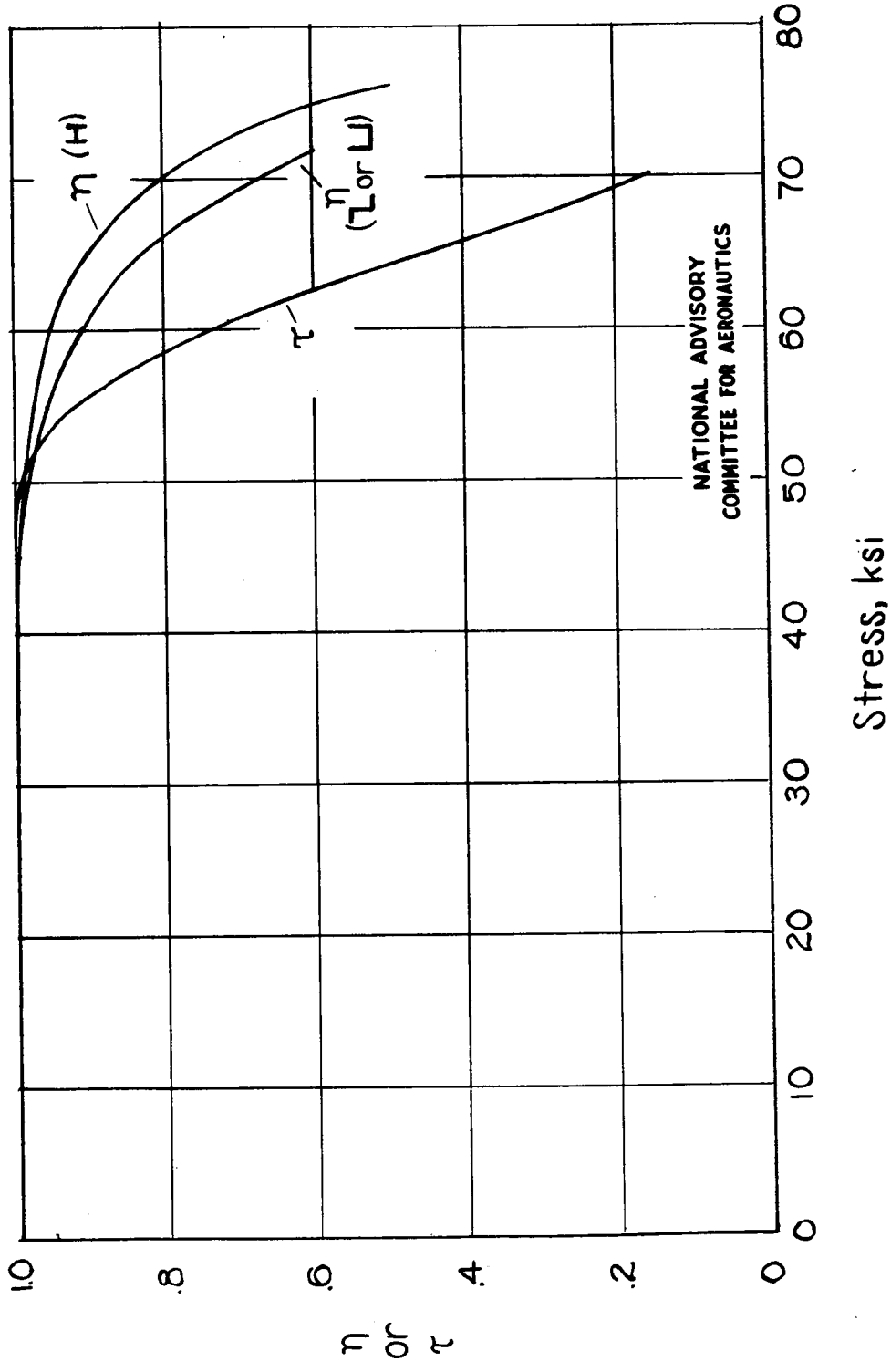

Figure 8.- Variation of τ and η with stress for extruded R303-T aluminum alloy. σ_{cy}(flange), 73 ksi; σ_{cy}(web), 71 ksi.

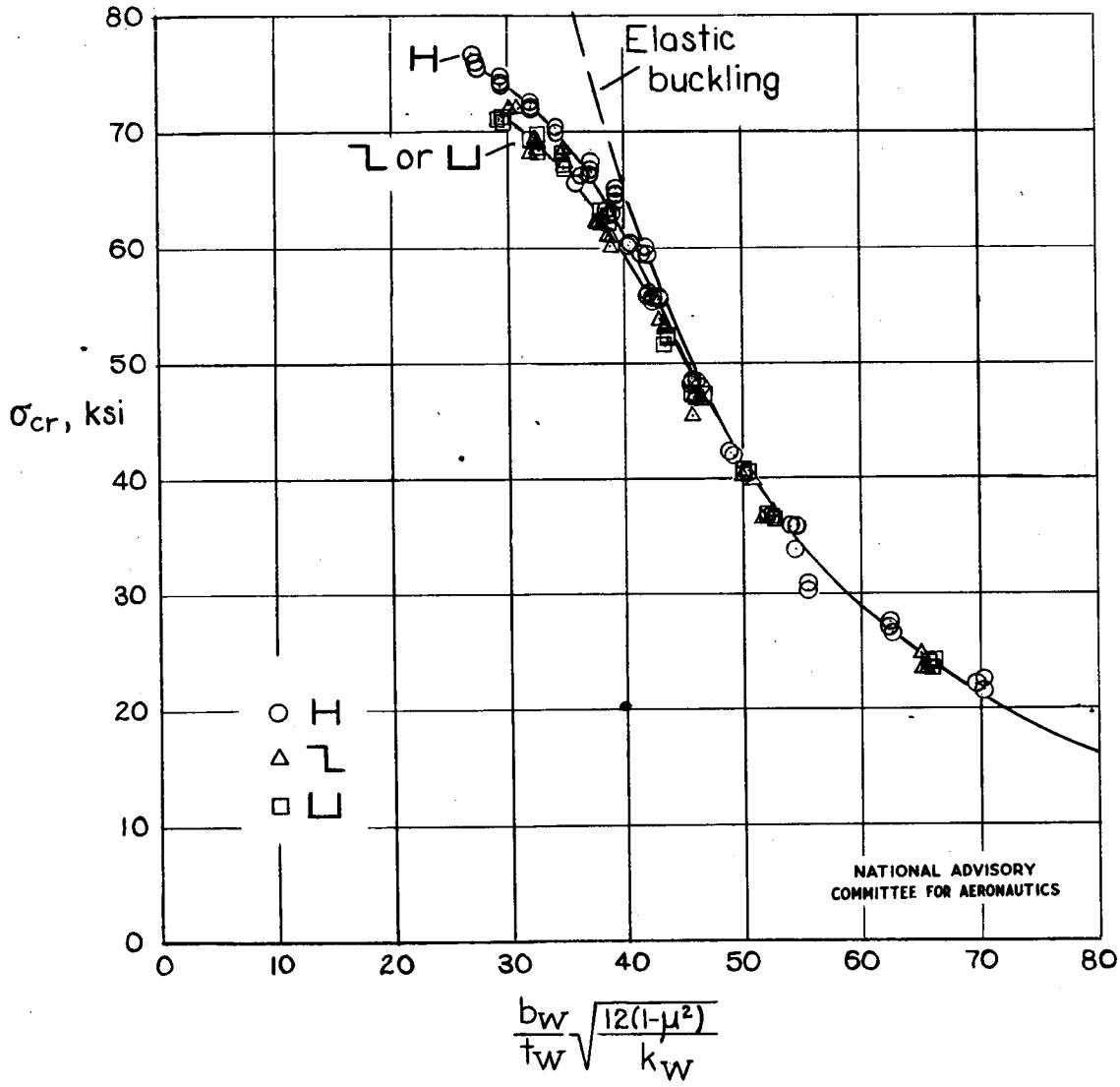

Figure 9.- Plate-buckling curves for extruded R303-T aluminum alloy obtained from H-, Z-, and channel-section columns. σ_{cy}(flange), 73 ksi ; σ_{cy}(web), 71 ksi.

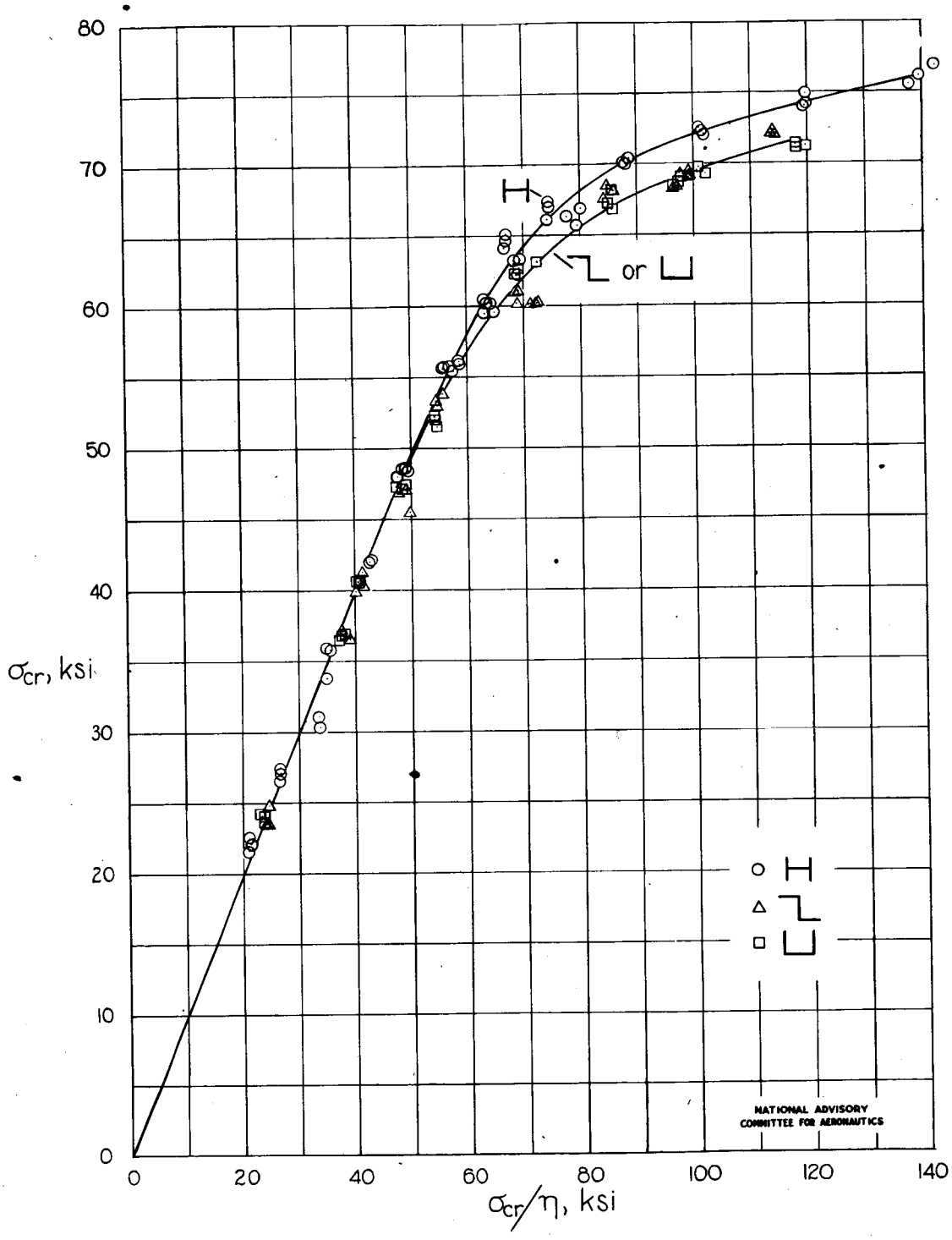

Figure 10.- Variation of σ_{cr} with σ_{cr}/η for plates of extruded R303-T aluminum alloy obtained from tests of H-, Z-, and channel-section columns. σ_{cy} (flange), 73 ksi ; σ_{cy} (web), 71 ksi .

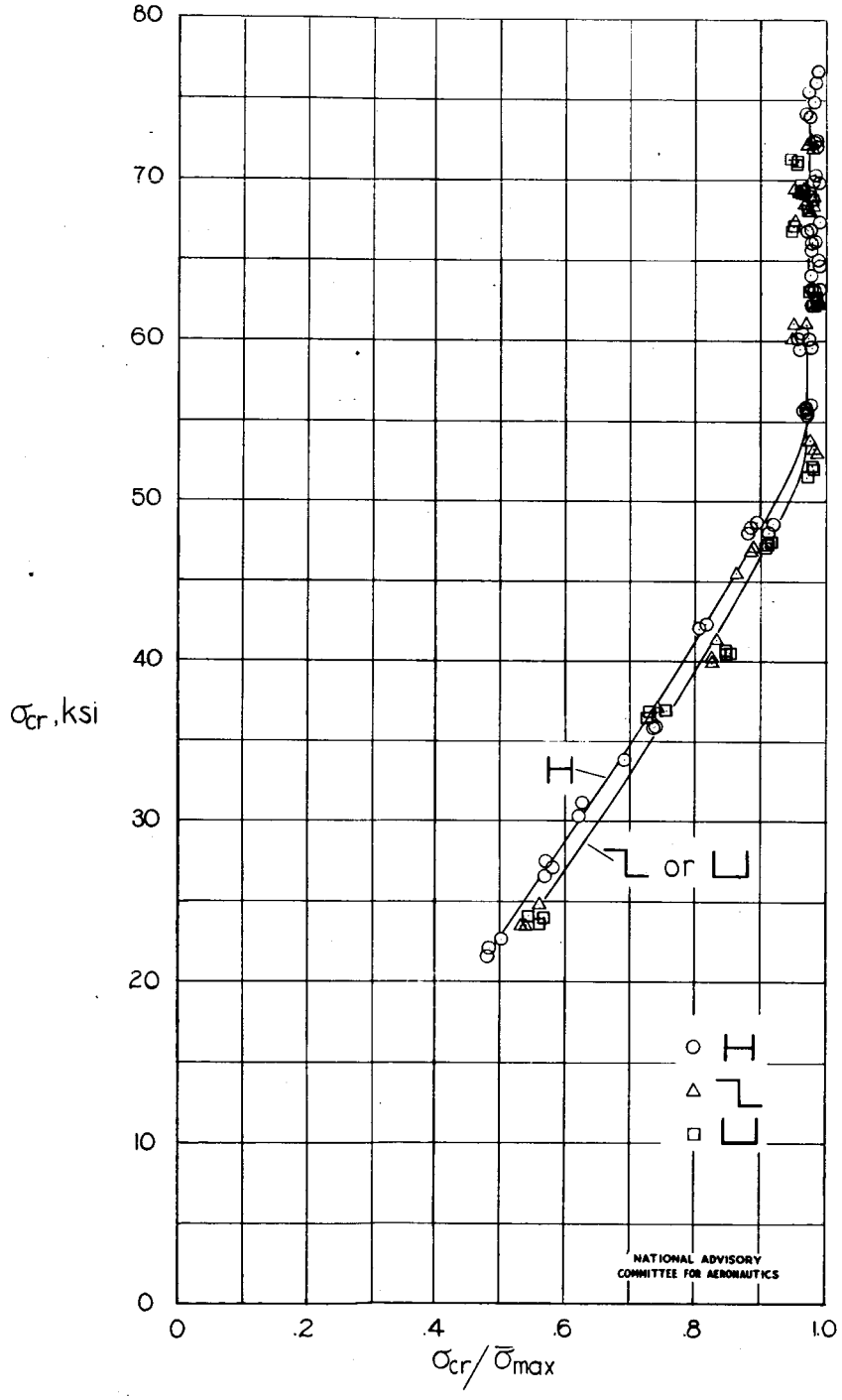

Figure 11.- Variation of σ_{cr} with $\sigma_{cr}/\bar{\sigma}_{max}$ for plates of extruded R 303-T aluminum alloy obtained from tests of H-, Z-, and channel-section columns. σ_{cy} (flange), 73 ksi; σ_{cy} (web), 71 ksi.

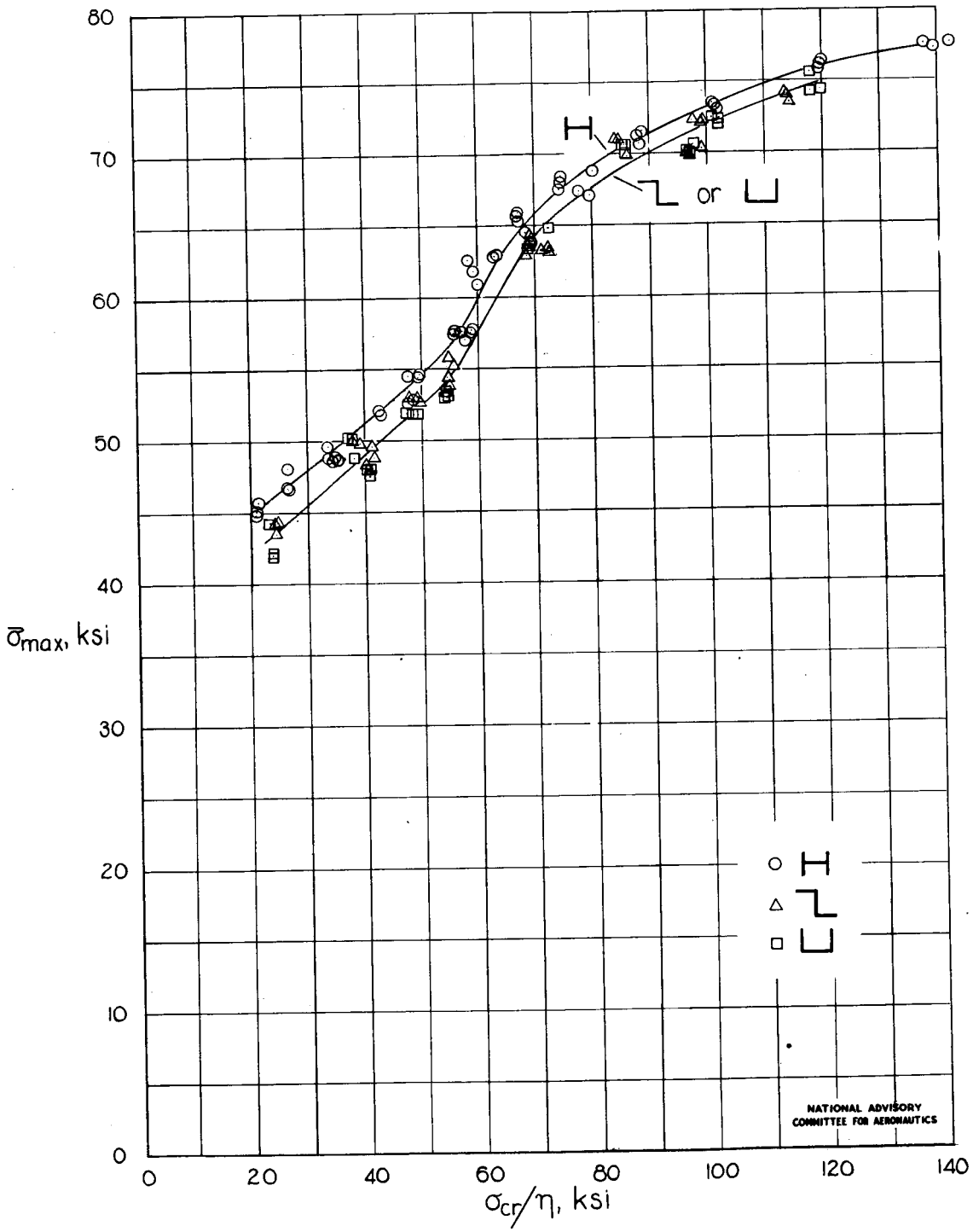

Figure 12.- Variation of $\bar{\sigma}_{max}$ with σ_{cr}/η for plates of extruded R303-T aluminum alloy obtained from tests of H-, Z-, and channel-section columns. σ_{cy} (flange), 73 ksi; σ_{cy} (web), 71 ksi.